Journal of Building Engineering 13 (2017) 184–195

Contents lists available at ScienceDirect

Journal of Building Engineering

journal homepage: www.elsevier.com/locate/jobe

An innovative anchoring system for old masonry buildings

J. Guerreiro*, A.S. Gago, J. Ferreira, J. Proença

Civil Engineering, Architecture and Geo-Resources Department, Instituto Superior Técnico – Universidade de Lisboa, Lisbon, Portugal

ARTICLE INFO

Keywords:
Anchoring system
Masonry walls
Rubble stone
Old buildings
Seismic reinforcement

ABSTRACT

The following paper presents the most recent results of a research programme carried out to, among other purposes, develop an innovative anchoring system for old masonry buildings. Despite the recognized importance of connections and anchoring systems, there is little experimental information about their strength and stiffness when installed in the masonry walls of old buildings. Therefore, one of the important goals of the research programme mentioned was the experimental characterization of the proposed anchoring system.

The main characteristic of the proposed system, which makes it different from others, is an internal spherical steel element where the rod is connected. This steel eleme nt, called hinge, allows no orthogonality between the steel anchor plate and the tie rod, which makes it suitable for uneven connections between orthogonal walls and/or walls and floors.

Besides this particular characteristic, the proposed system demonstrates all the capabilities of the traditional anchoring systems, namely, it can be used to strengthen the connection between orthogonal masonry walls or to ensure the connection of constructive elements (floors, roofs, stairs, etc.) to masonry walls.

Moreover, numerical simulations with non-linear finite elements models were performed, aimed at reproducing the experimental tests for other load conditions or different wall thicknesses.

The prime objective of the experimental and numerical studies was to assess the actual behaviour of the anchoring system and to establish appropriate design rules, which are also presented in this paper.

1. Introduction

The proprietary anchoring system discussed in this paper, developed by STAP, S.A (www.stap.pt) with the scientific support of the CERIS (www.ceris.pt), was designed with the purpose of preventing the out-of-plane collapse of masonry walls in old buildings, ensuring in this way a global behaviour of the building.

It is well known that the deficient structural behaviour of old masonry buildings when hit by an earthquake is mainly due to the insufficient strength of the connections between walls and between walls and floors. When good connections are provided, the masonry building behaves globally, like a three-dimensional “box”, where masonry walls work, essentially, in its plan, increasing the global seismic strength of the building [1]. Thus, any technique which improves the strength of the connections (or that establishes effective connections) between orthogonal walls and between walls and floors, would result in a significant increase of the building's seismic strength [2,3].

The implementation of anchoring systems in masonry walls is not a novelty, nor is the connection of wooden floors to masonry walls [4–6]. Those systems began to be added from the beginning of the masonry buildings [7], initially with wood or cast iron elements and, more recently, using steel plates and steel tie rods. However, although the benefits of these systems in masonry constructions are well known, their design, though, is not always easy, due to the lack of experimental data.

Despite the availability of some experimental studies for anchor plates in brick masonry [8–11], for traditional rubble stone masonry walls (irregular stone bonded with air lime mortar) experimental data is scarce [12]. Nevertheless, it must be mentioned that in the development of the system presented herein, other experimental tests using rubble stone masonry specimens [13] have been performed to characterize the strength of "wooden elements” connections” - masonry walls.

Thus, one of the main goals of the current present research programme is to experimentally assess (by pull-out tests) the strength and the mechanical behaviour of the proposed anchoring system, when applied to traditional rubble stone masonry walls. Moreover, numerical simulations with non-linear models of finite elements were performed with the aim of reproducing the experimental tests for other load conditions. Finally, the results of the experimental and numerical tests were used to establish design rules for the proposed anchoring system, which are presented in Section 7.

* Correspondence to: CERIS, Av. Rovisco Pais, 1049-001 Lisbon, Portugal.
E-mail address: jg@civil.ist.utl.pt (J. Guerreiro).

http://dx.doi.org/10.1016/j.jobe.2017.08.002
Received 15 March 2017; Received in revised form 29 June 2017; Accepted 2 August 2017
Available online 04 August 2017

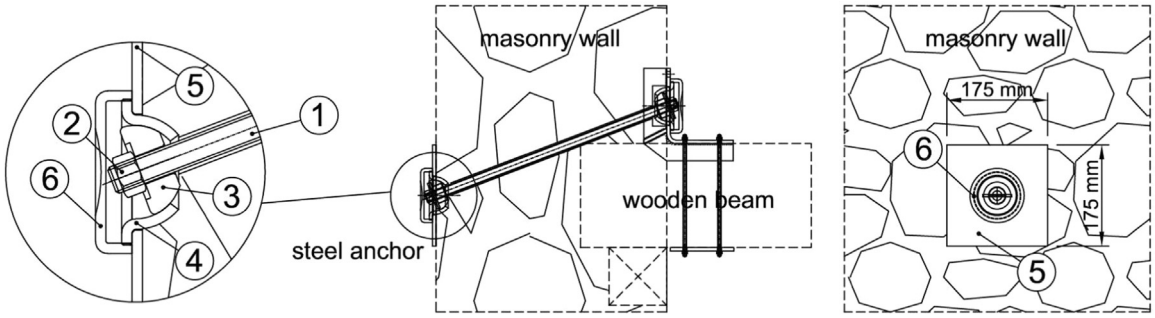

Fig. 1. Proposed anchoring system (wall-floor connection). **1** Tie rod. **2** Screw nut. **3** Steel hinge. **4** Steel cup. **5** Steel plate. **6** Steel cover.

2. Description of the anchoring system

The proposed anchoring system is composed of an anchor steel plate (175 × 175 × 6 mm3), connected to a steel cup (6 mm thick) and a steel hinge, which is connected, by a nut, to the steel tie rod (Fig. 1). The particularity of this system is the potentially tilted installation of the tie rod (up to an angle of 20°), rather than being placed horizontally. Due to the durability requirements that are now compulsory for the strengthening of old buildings, the anchoring system, as well as its tie rod, were designed in stainless steel (class Aisi 304. St70). A steel cover was added to the anchoring system in order to protect the nut and the steel tie rod, to provide permanent access. The steel cover has no effect on the system's mechanical performance.

3. Material characterization

The anchoring system was first of all tested to establish the diameter of the steel tie. The collapse of the anchoring system was meant to happen by the tie and not by the steel hinge itself. Tensile tests to the anchoring system were performed (Fig. 2.a), in accordance with the following the procedures of the ASTM E8 standard [14] for the tension testing of metallic materials. Three tensile tests were done for the system with a M20 stainless steel tie rod, achieving a maximum load (mean value) of 200 kN, provided by the tie rod collapse (Fig. 2.b). With regard to the stiffness of the system, it is worth noting that the deformability of the steel hinge was not significant, when compared to the M20 rod deformability.

The rubble stone masonry specimens used for the experimental test process needed preliminary material characterization. Among other aspects, special attention was given to the following variables:

- Limestone - uniaxial compressive strength, in accordance with the EN 1926 European Standards [15];
- Mortar - compressive and flexural strength, in compliance with the EN 1015-11 Eurpoean Standards [16];
- Mortar - age evolution of its mechanical properties [17];
- Masonry - uniaxial compressive strength, in line with the EN 1015-11 European Standards following the EN 1052-1 proceedings [18];
- Masonry - compressive strength of two-leaf masonry specimens.

Three cylindrical samples (Ø63 mm × 70 mm height) were cored from stone blocks used to build the specimens, which were tested to evaluate their compressive strength (Fig. 3). From these tests, a uniaxial compressive strength of 51 MPa (mean value) was obtained.

Forty-five mortar prismatic specimens (40 × 40 × 160 mm3) were made and tested in line with the EN 1015:11 European Directives. [16]. From these tests, a mortar compressive strength of 1.76 MPa was obtained from 28-day-old specimens and a mortar tensile (flexural) strength of 0.46 MPa (Table 1). For specimens, 42 and 168 days old, a compressive strength of 1.65 and 2.36 MPa (respectively, Table 1) was obtained and a tensile (flexural) strength of 0.43 and 0.44 MPa (respectively, Table 1). Mortars had a high percentage of clay-rich sand in their composition (about 50% on of its mass constitution), and this composition could be the reason for the dependency between the compression strength and the age of the mortar.

It is well known that masonry properties do not depend exclusively on their materials. In fact, the way the stone is "neat" while laying up the masonry walls, the size and shape of the stones, the mortar joints' thickness and the stiffness ratio between mortar and stone, as much are just as important as the material's mechanical properties. Therefore, uniaxial compression tests were carried out on fifteen cubic (40 × 40 × 40 cm3) masonry specimens, all 70 days old (Fig. 4). For these specimens, built with the stone and mortar previously described, an average failure stress of 2.41 MPa was achieved (with a standard

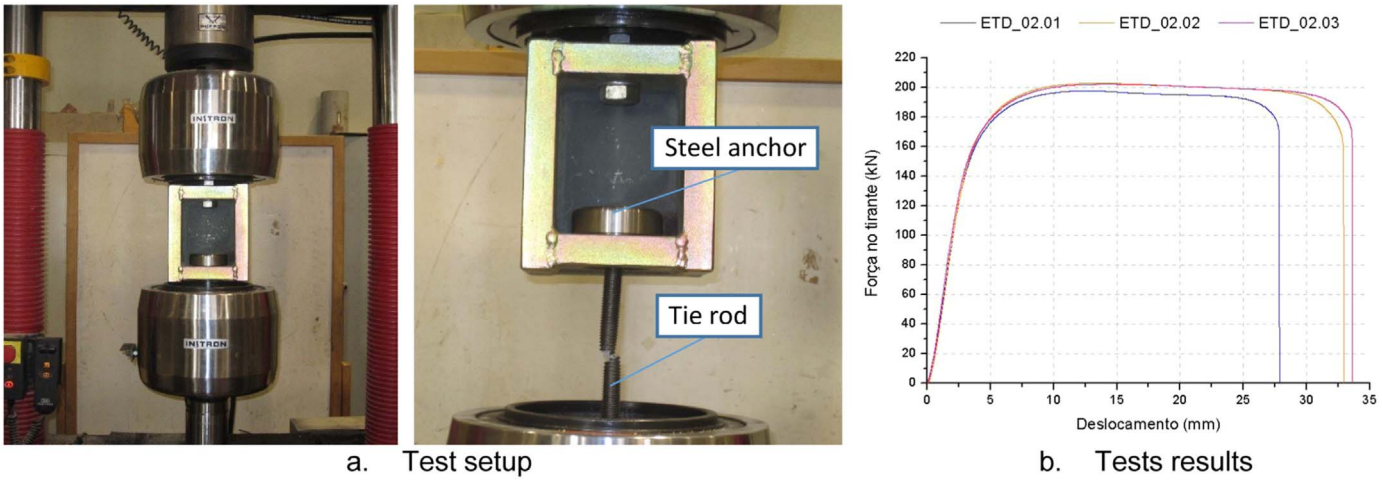

a. Test setup b. Tests results

Fig. 2. Direct tensile tests performed to the anchoring system.

Fig. 3. Limestone uniaxial compressive tests.

Table 1
Mortar (compressive and flexural) strength.

	COMPRESSION RESISTANCE - σ_c		FLEXURAL RESISTANCE - σ_F	
SAMPLE AGE AT TEST	AVERAGED STRESS	STANDARD DEVIATION	AVERAGED STRESS	STANDARD DEVIATION
28 days	1.76 MPa	7.35%	0.46 MPa	5.61%
42 days	1.65 MPa	3.33%	0.43 MPa	3.24%
168 days	2.36 MPa	8.13%	0.44 MPa	4.09%

deviation of 19.31%) and a Young modulus of 1.3 GPa.

To study the influence on the masonry strength of the specimens' size, morphology (i.e. number of leaves) and specimens' age, six 120 × 120 × 40 cm3 sized specimens were built and tested in compression. The specimens were built with two stone leaves, applying the same mortar and technique used in the previous masonry specimens. Three of the two-leaf specimens were tested when they reached 125 days old (PAV_01 to PAV_03) and the remaining three specimens that were 60 days old (PAV_06 to PAV_09). For the older specimens a maximum force of 904 kN (average figure) was obtained (Fig. 5), while for the younger specimens, a maximum force of 395 kN (mean value) was achieved (Fig. 6).

Experimental tests were numerically reproduced by non-linear finite element models (MC_01 and MC_02, Fig. 7, for details of the numerical model, see Section 6). For the finite elements models, two different Constitutive Laws were adopted: one (MC_01 model) with a compression strength of 1.80 MPa, a tensile strength of 0.15 MPa and a Young modulus of 1.00 GPa; and the other (MC_02 model) with a compression strength of 3.20 MPa, a tensile strength of 0.20 MPa and a Young modulus of 2.00 GPa. Similar values were also used in other studies [19] and a good agreement was achieved for both the younger specimens (MC_01 model) and the older specimens (MC_02 model). Fig. 7 lays out the experimental and numerical "force-displacement" curves, as well as the maximum principal stresses of the numerical models immediately before the collapse.

Regarding the concentration of anchoring systems applied in a masonry wall and their effect on the compression behaviour of the specimens, three specimens were tested (PAV_04, PAV_05 and PAV_09), each one strengthened with 9 anchoring systems (Fig. 8). The specimens were 60 days old and the anchoring systems were applied in a 40 cm square mesh (corresponding to the thickness of the wall). The maximum vertical load (average value) was 443 kN, slightly higher than the value obtained with the masonry specimens, 60-days-old.. However, since the collapse no longer included the two leaf separation (Figs. 6.a and 8.a), an increase in the specimens' deformation capacity was noted.

Therefore, the introduction of anchoring devices does not exactly increase (or decrease) the masonry compression strength but leads to an increase in the deformation capacity.

With the previous materials' characterization, a mortar composition and a procedure to build the masonry was possible to establish, which led to specimens with similar characteristics to the typical Portuguese (and Mediterranean) rubble stone masonry walls [12,13,19,20]. The last set of characterization tests enabled us to understand that the use of these anchoring systems does not significantly influence the compression strength of the masonry walls.

4. Experimental setup

The development of the anchoring system needed an experimental study to define/outline/identify the pull-out strength of the anchoring

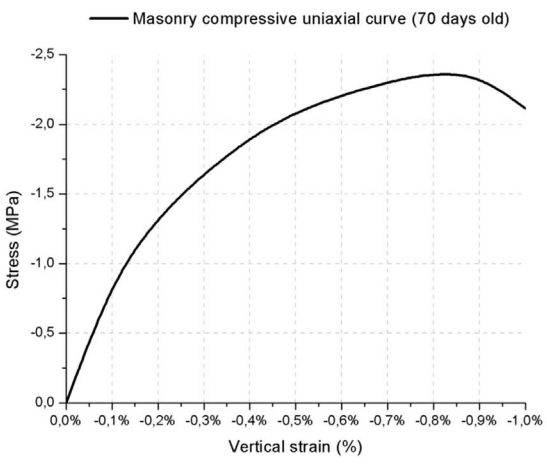

Fig. 4. Masonry uniaxial compressive strength.

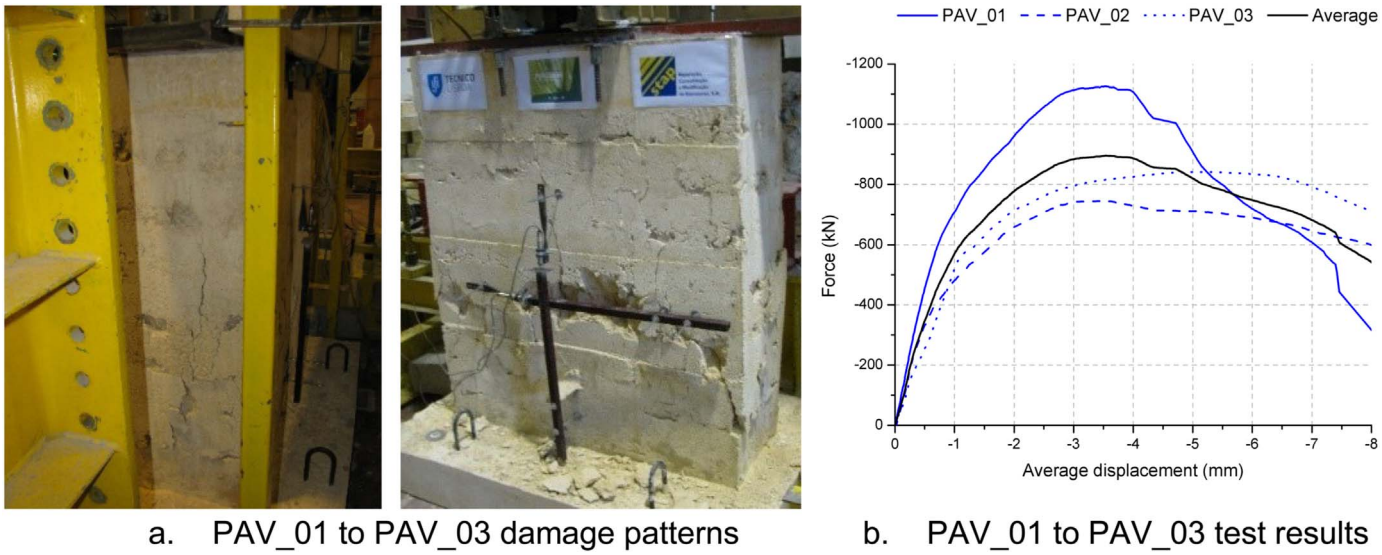

Fig. 5. Wall compression tests (non-confined walls – 125 days old).

system when installed in a rubble masonry wall. Hence, a total of twelve pull-out tests were performed (Table 2), varying the applied in-plane load and the bore-hole tilt.

The twelve 120 × 120 × 40 cm^3 masonry specimens were made using the materials and techniques established in the previous section and were tested when 60 days old. Each masonry specimen was placed horizontally over a wooden substrate (Fig. 9), which was designed to be stiff enough to have no influence on the specimen's behaviour when the anchor rod was pulled. The wooden substrate had an 80 × 80 cm2 opening (Fig. 9), provided to avoid any influence on the punching surface generation.

Two anchoring systems were applied in the specimens, one on the upper surface and another on the bottom surface, which enabled us to put the tie rod setting with the desired inclination (0° to 20°). The pull-out force was applied to the anchor located on the bottom surface (by a switch-over piece - Figs. 9 and 10), perpendicularly to the specimen's surface.

The pull-out force was applied to the tie rod by a 200 t hydraulic jack, to which a 200 kN load cell was coupled. The specimens' displacements were measured by three transducers, two of them located on the bottom surface (transducers 6, Figs. 9 and 10) and one over the upper anchoring system (transducer 5, Figs. 9 and 10).

To simulate the effect of compression stress that masonry walls are subjected to (due to their own weight and other gravity loads), in-plane stresses were applied to the specimens by a system of hydraulic jacks and ties (Fig. 10). Three levels of in-plane stress were considered:

I. Zero compression stress;
II. Compression stress of 0.21 MPa (by a 100 kN in-plane load) - to simulate walls at a higher floor level;
III. Compression stress of 0.50 MPa (by a 240 kN in-plane load) - to simulate walls at ground floor level.

To faithfully reproduce the actual application conditions of he anchoring systems, the anchors were installed when the above-mentioned confining in-plane stress was applied.

To estimate the maximum pull-out force for the anchoring system (Table 2), three sets of tests were performed. The first set was performed without any in-plane stress and a monotonic loading protocol (PAH_01 to PAH_03, Table 2). A force-controlled loading cycle

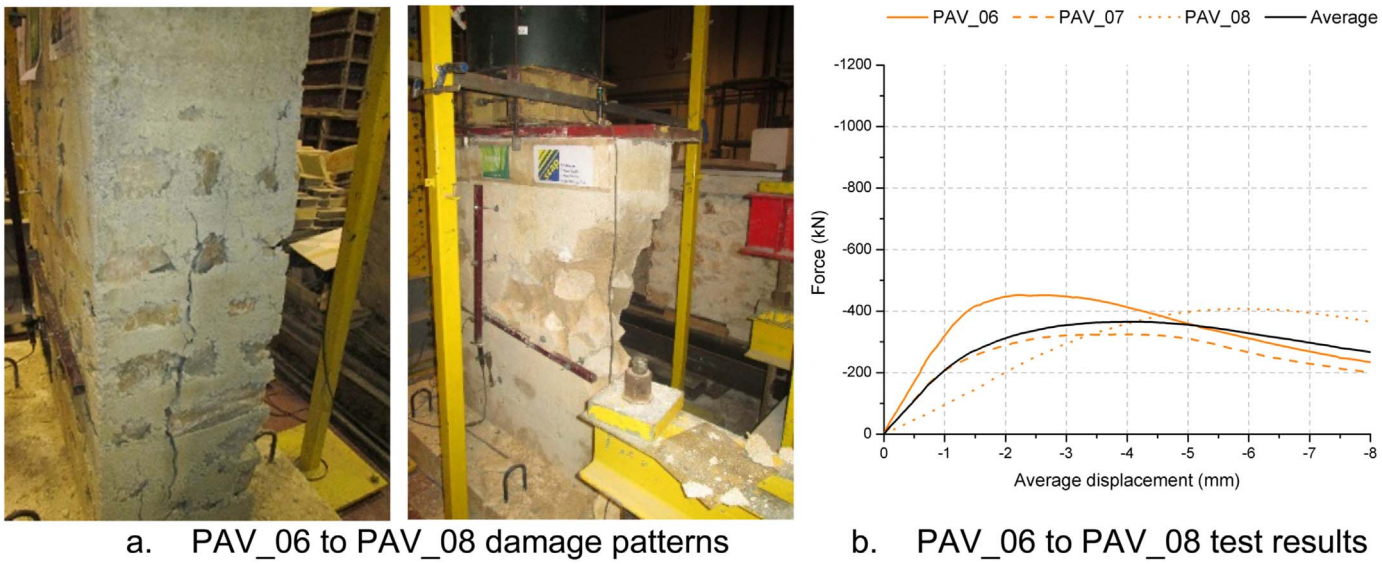

Fig. 6. Wall compression tests (non-confined walls – 60 days old).

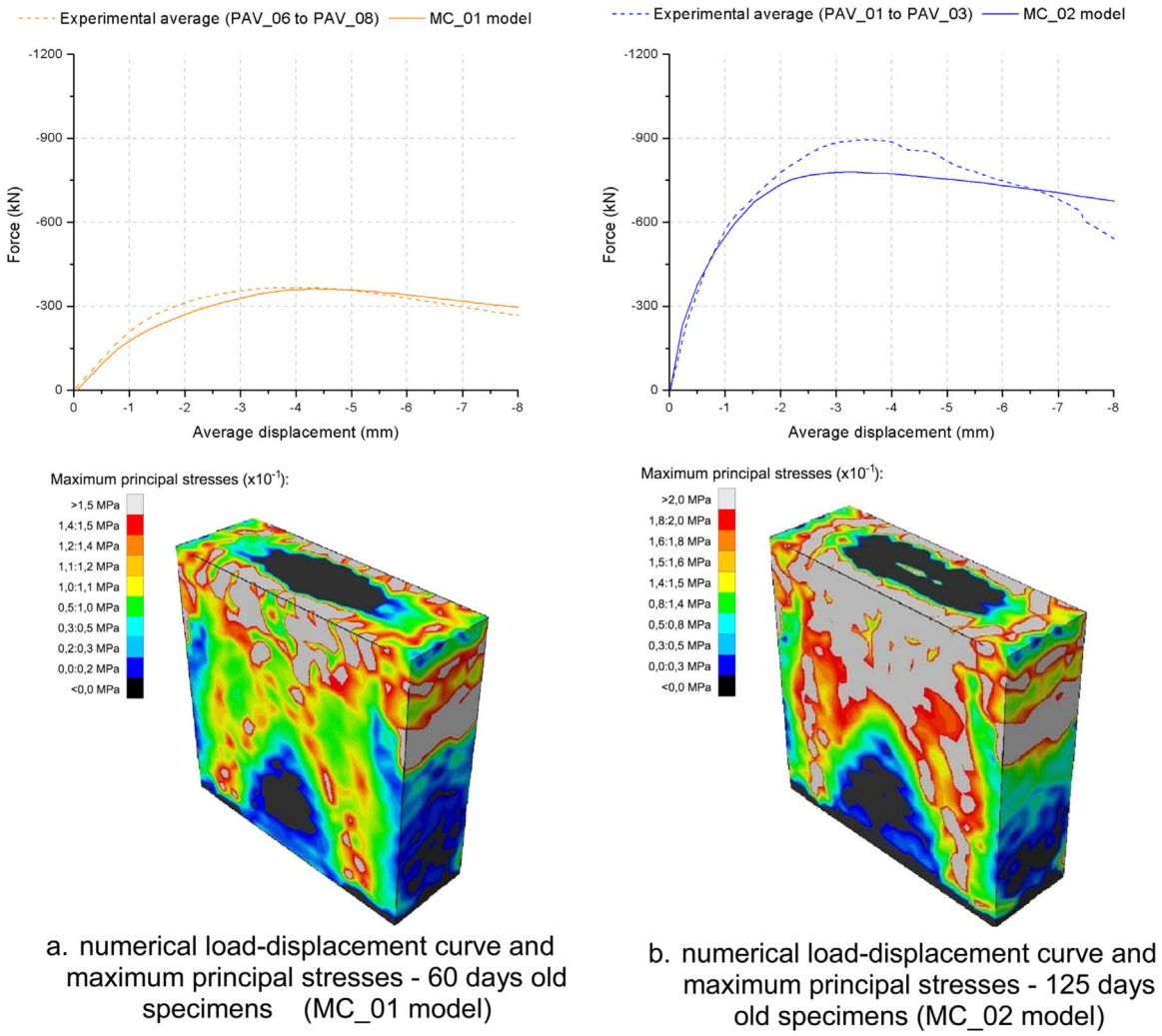

Fig. 7. Masonry walls properties numerical calibration.

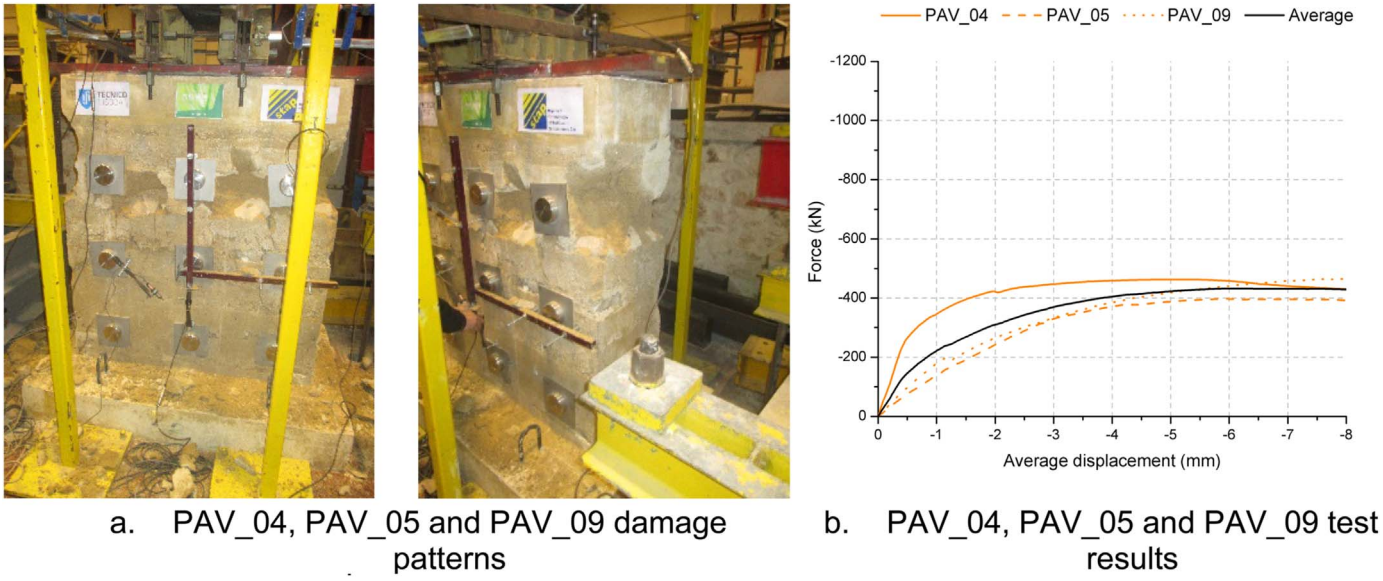

Fig. 8. Wall compression tests (confined walls – 60 days old).

Table 2
Anchor pull-out tests distribution.

TEST REF.	TEST RHYTHM	IN PLANE LOADING FORCE (STRESS)	BORE-HOLE INCLINATION	MAXIMUM PULL-OUT FORCE		
				LOAD (KN)	MEAN VALUE (KN)	STD. DEVIATION
PAH_01	Monotonic	Without in plane load	Perpendicular to the wall leafs	42.1	46.67	9.66%
PAH_02				45.1		
PAH_03				52.8		
PAH_04	Cyclic (following Fig. 9 load cycle)	100 kN (0.21 MPa)	Perpendicular to the wall leafs	110.9	106.40	13.96%
PAH_06				81.8		
PAH_07				111.2		
PAH_08				121.7		
PAH_09	Cyclic (following Fig. 9 load cycle)	240 kN (0.50 MPa)	Perpendicular to the wall leafs	121.3	115.10	7.88%
PAH_10				120.1		
PAH_11				109.9		
PAH_12			20° to the wall normal	99.8		
PAH_13				124.4		

(Fig. 11), with two returns for each force step of 10 kN was used in the second set (PAH_04 to PAH_08, Table 2).

For the tests on the second set, the tie was always perpendicular to the specimens' surfaces (i.e. with an angle of 0° with the normal to the surfaces) and an in-plane stress of 0.21 MPa was applied. The third set was performed with a 0.50 MPa in-plane stress, with the same force-controlled loading cycle and with two layouts for the tie rod: 0° with the normal to the surfaces (PAH_09 to PAH_11, Table 2) and 20° with the normal to the surfaces (PAH_12 and PAH_13).

5. Experimental results

In the monotonic tests (specimens PAH_01 to PAH_03) conducted without any in-plane load, two types of damages were identified. First, for a displacement level of about 3–4 mm (and corresponding to a peak value of the applied pull-out force, Fig. 12.b) two external cracks appeared (Fig. 12.a), resulting in a decrease of strength in the specimens. Then, from a displacement of about 5 mm, a hardening behaviour was observed, until the moment where the punching shear surface was damaged and the failure occurred.

Subsequent tests were carried out with in-plane loading (of 0.21 and 0.50 MPa) and with a cyclical pushing load. The first type of damage occurred in the previous tests (and the corresponding peak value of the force no longer happened) and the collapse occurred with a clear formation of the punching shear cone. For the specimens with smaller in-plane stresses (0.21 MPa, specimens PAH_04 to PAH_08), it was observed, at the collapse, the penetration of the steel plate of the system into the masonry substrate was noted (Fig. 13.b), while a punching shear cone (with a surprisingly regular shape) was simultaneously formed (Fig. 13.a).

For the early loading stages, all the specimens presented similar behaviour (Fig. 14). For higher loads, differences appeared due to the different deformability of the masonry below the steel plate. It was recognized that the way the steel plate penetrated into the masonry had an important influence in the system capacity (strength and deformability).

For the specimens tested with the lowest in-plane stress (0.21 MPa) the anchoring system achieved a pull-out resistance of 106.4 kN (mean value – see Table 2).

The failure type of the specimens tested with the lowest level of in-plane stress was also seen in the specimens tested with the highest level of in-plane stress (0.50 MPa, PAH_09 to PAH_13). However, the punching surface had a semi-circular generation line in the in-plane loading direction, instead of a linear one (Fig. 15.a). In addition to this failure mode the separation of the masonry leafs was also observed (Fig. 15.b) after the complete formation (and detachment) of the punching cone.

In specimens PAH_12 and PAH_13, the tie rod was placed with a 20° angle between the tie and the normal to the specimens' surface. The results gathered (Fig. 16) and the specimens' behaviour showed that the tie rod angle had no relevant influence on the pull-out capacity of the anchoring system. For the specimens tested with the highest in-plane stress (0.50 MPa), the anchoring system achieved a pull-out resistance of 115.1 kN (average value – see Table 2).

6. Numerical modelling

The primary goal of the numerical studies' was to develop a model

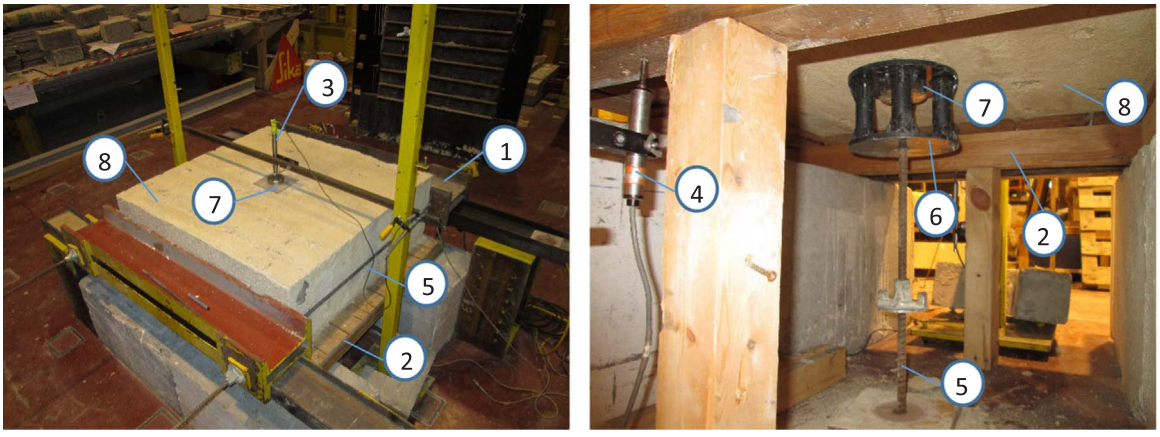

Fig. 9. Anchor pull-out test assemblage. **1** Distribution beam. **2** Wooden substrate. **3** Disp.transducer. **4** Disp. transducer. **5** Diwydag bar. **6** Switch-over piece. **7** Anchoring system. **8** Masonry specimen.

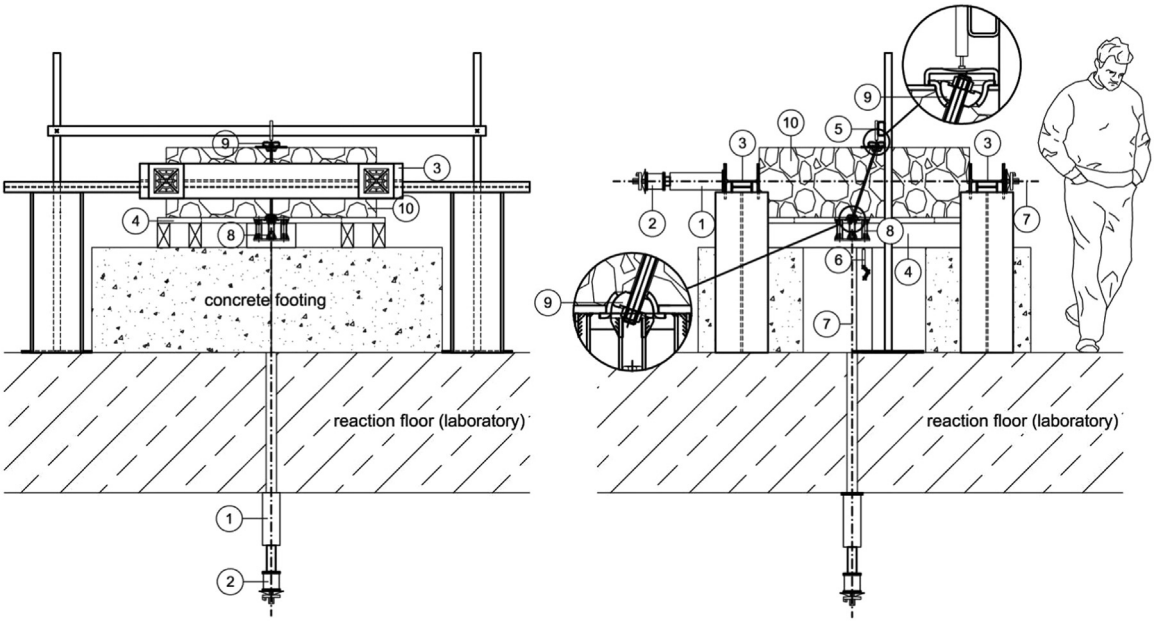

Fig. 10. Anchor pull-out tests setup. **1** Hydraulic jack. **2** Load cell. **3** Distribution beam. **4** Wooden substrate. **5** Disp.transducer. **6** Disp. transducer. **7** Diwydag bar. **8** Switch-over piece. **9** Anchoring system. **10** Masonry specimen.

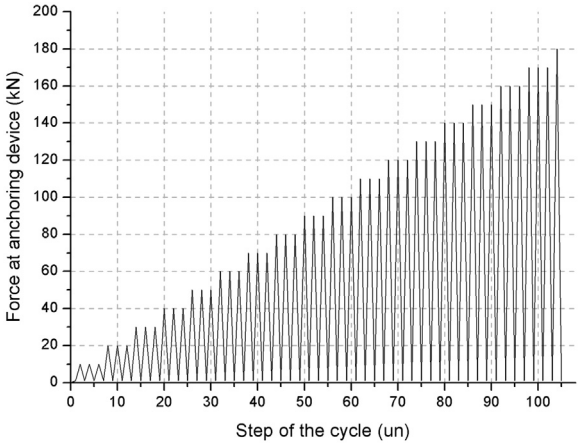

Fig. 11. Pull-out tests load cycle.

to be used to simulate other test conditions, namely different masonry strengths and different levels of in-plane loading. Other cases, like the different dimensions of the anchor steel plate, could further be tested with the numerical model.obtained.

In order to obtain a reliable numerical model, a careful calibration was made, first of all, the results of the simplest performed tests (i.e., the compression tests) and, later on, the results of the cyclic pull-out tests.

As mentioned in Section 3 (see Fig. 7), the compression tests were well reproduced by non-linear finite element models (10 nodes solid tetrahedron elements), with a Young modulus of 2.00 GPa (125 days old specimens) or 1.00 GPa (60 days old specimens), a compression strength of 3.20 MPa (125 days old specimens) or 1.80 MPa (60-day-old specimens) and a tensile strength of 0.20 MPa (125 days old specimens) or 0.15 MPa (60 days old specimens). The previous mechanical parameters were considered in the constitutive laws adopted for the finite elements, which are depicted in Fig. 17.

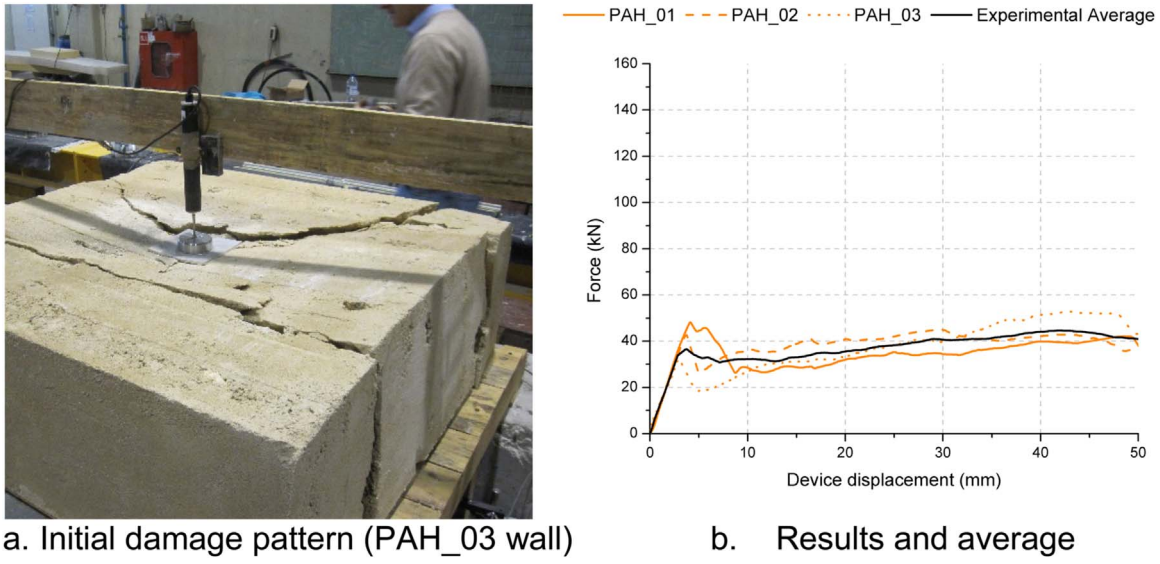

Fig. 12. Cyclic pull-out tests (without in-plane loading).

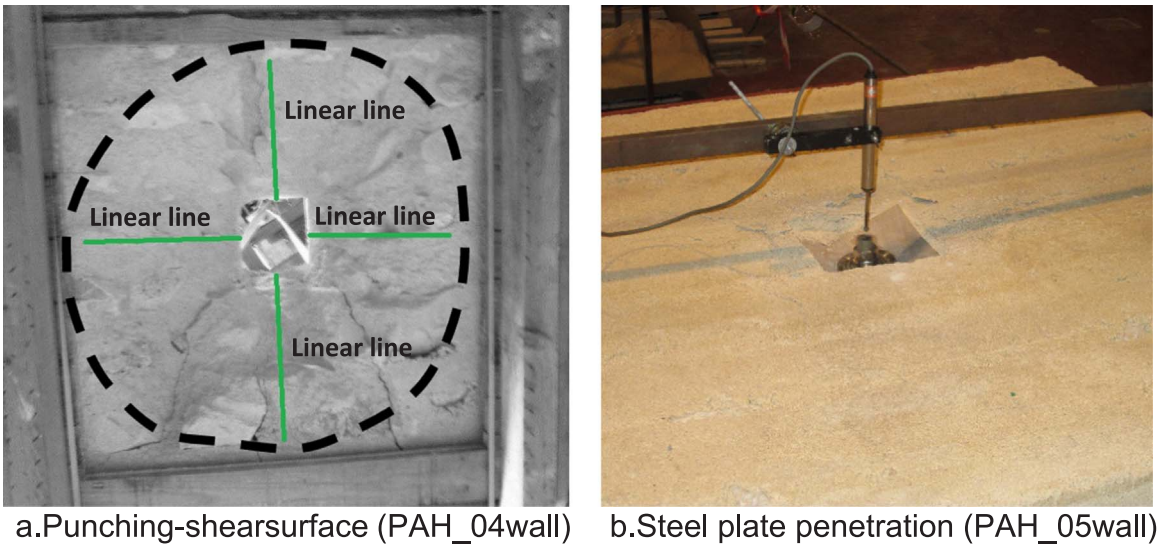

Fig. 13. Cyclic pull-out tests damage patterns (in-plane load of 100 kN / 0.21 MPa). a. Punching-shear surface (PAH_04 wall). b. Steel plate penetration (PAH_05 wall).

The same elements and Constitutive Laws previously used for the simulation of the compression tests were also used for the pull-out tests' simulation. Several simulations of the pull-out tests were performed and a positive match was obtained (Fig. 18). Simultaneously, a parametrical study was also performed in order to understand the effects of the in-plane load as well as the masonry strength (Table 3). The numerical results gathered were used to calibrate the design rules laid out in Section 7.

To understand the in-plane load effect, numerical tests were performed with four levels of in-plane stresses (Table 3): 0.21 and 0.50 MPa, corresponding to the experimental tests, an intermediate level of 0.35 MPa and a higher level of 0.75 MPa.

Numerical tests were also performed based on a tensile strength 50% higher than the calibrated value for the specimens that were 125 days old (i.e. 0.30 MPa), while the remaining mechanical characteristics were kept unchanged. The goal of this new material (hereafter referred to as 125 + days) was to simulate a stronger material, for instance, stone masonry bonded by a hydraulic lime mortar, which presents a higher tensile strength than the typical stone masonry with an air lime mortar binder.

The results of the numerical simulations are illustrated in Figs. 18 and 19, a close correlation with the numerical and experimental load-displacement curves can be seen. The maximum principal stresses depicted in Fig. 18 (obtained immediately before the load failure) are also in accordance with the shape of the experimental punching surfaces (Fig. 18.c).

The parametric study made it clear that for in-plane load levels above a certain amount, the increment in the pull-out capacity is not relevant (Figs. 18 and 19). For instance, for a 125 days old masonry, the pull-out capacity will not significantly increase after an in-plane stress of 0.20 MPa.

Moreover, it was noted that the pull-out capacity is sensitive to the

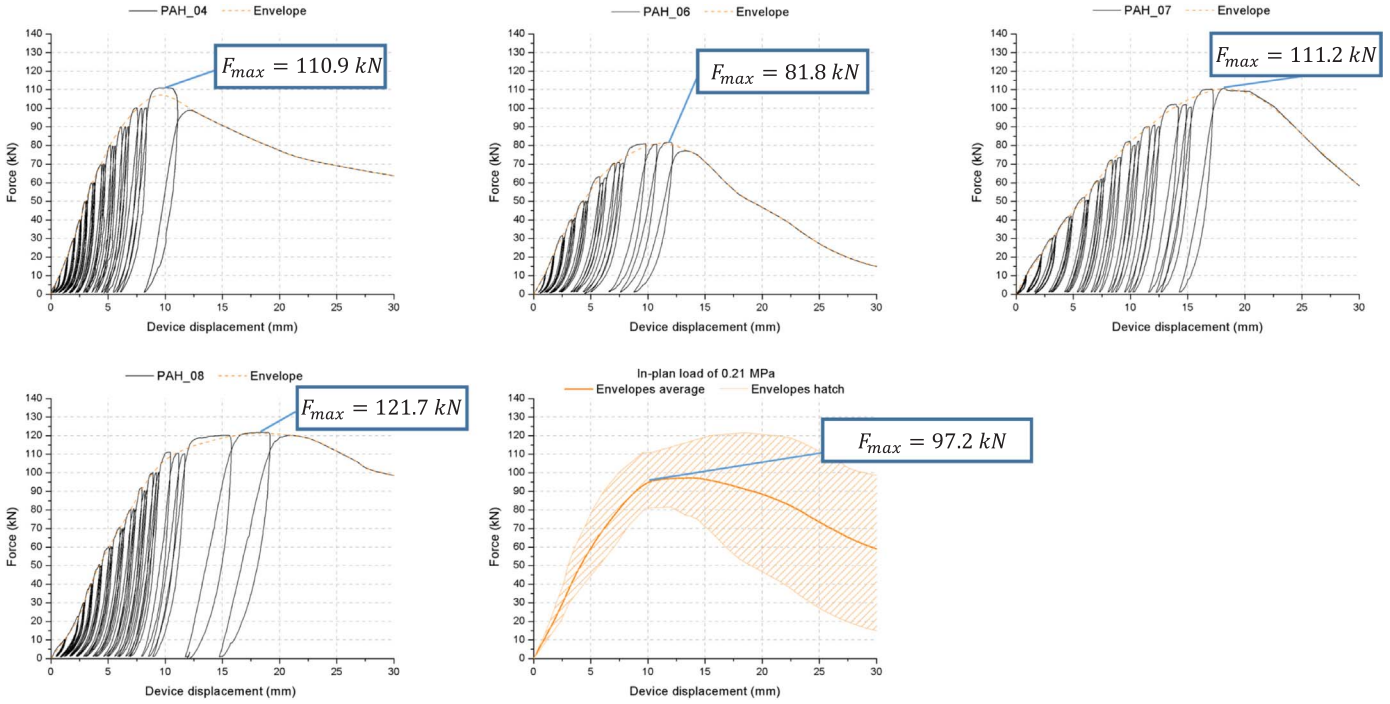

Fig. 14. Cyclic pull-out tests results (in-plane load of 100 kN /0.21 MPa).

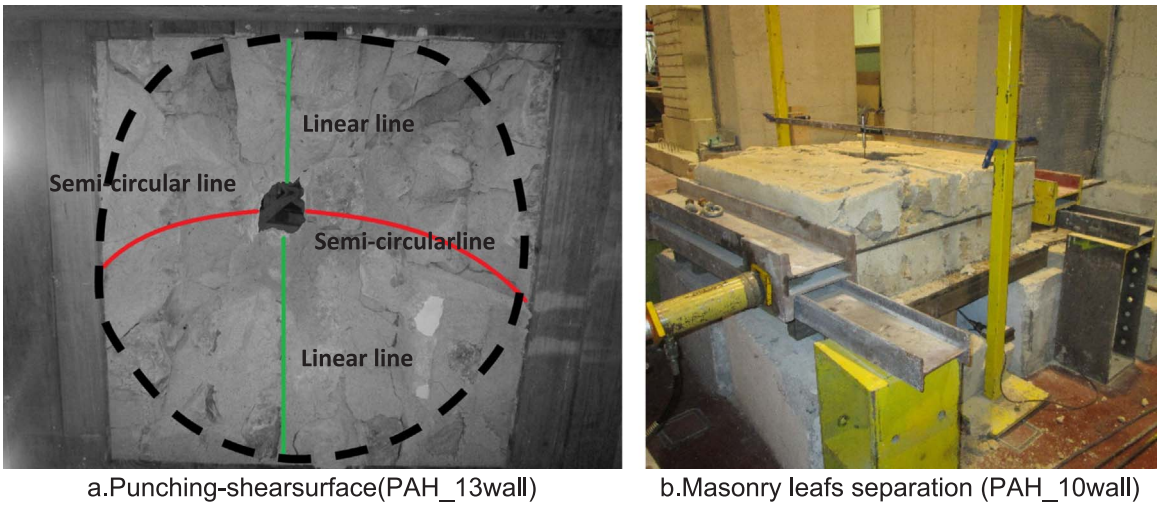

Fig. 15. Cyclic pull-out tests damage patterns (in-plane load of 240 kN / 0.50 MPa).

masonry strength (tensile and compression strength) and, therefore, that issue should be considered in the analytical model to evaluate the anchoring system pull-out capacity. From the numeric results, it can also be stated that the anchoring system deformability is a result of the behaviour of the anchoring system itself (i.e. to the tied rod), as all the numerical models showed, approximately, the same elastic stiffness.

7. Design rules

One of the principal goals of the present research was the development of design rules for the proposed anchoring system. That process was based on the reproduction of the experimental and numerical results, i.e., on the bilinear "pull-out capacity vs. applied in-plane stress" interpolation curves illustrated in Fig. 20.

The fact that the punching collapse happens when the maximum principal stress reaches the masonry tensile resistance can, therefore, be acknowledged. Given that in the absence of in-plane loading, the punching cone surface follows the masonry friction angle and a simple design rule (1) for the pull-out capacity can be established:

$$F^{1}_{a,R}(h, \phi, \sigma_t) = S_{cone}(h, \phi) \times \sigma_t \times \text{sen}\phi \quad (1)$$

Where $F^{1}_{a,R}$ is the pull-out capacity when no in-plane load is applied, h the wall thickness, ϕ the masonry friction angle, σ_t the masonry tensile resistance and S_{cone} the lateral surface area of the regular pushing cone (Fig. 21), superiorly cut by the steel plate (175 × 175 mm^2).

For an in-plane loaded (σ_n) wall, the masonry internal stresses have a different pattern and the shape of the punching surface is dependent on the magnitude of the in-plane load (until a certain level of in-plane loading is reached). However, instead of looking for the exact shape of the punching surface, the basic surface defined above was taken into consideration, affecting the results by a coefficient λ_1 which takes into account the effects of the in-plane compression. The obtained design rule obtained for the pull-out capacity of the anchoring system in compressed walls $F^{2}_{a,R}$ is presented in Eq. (2):

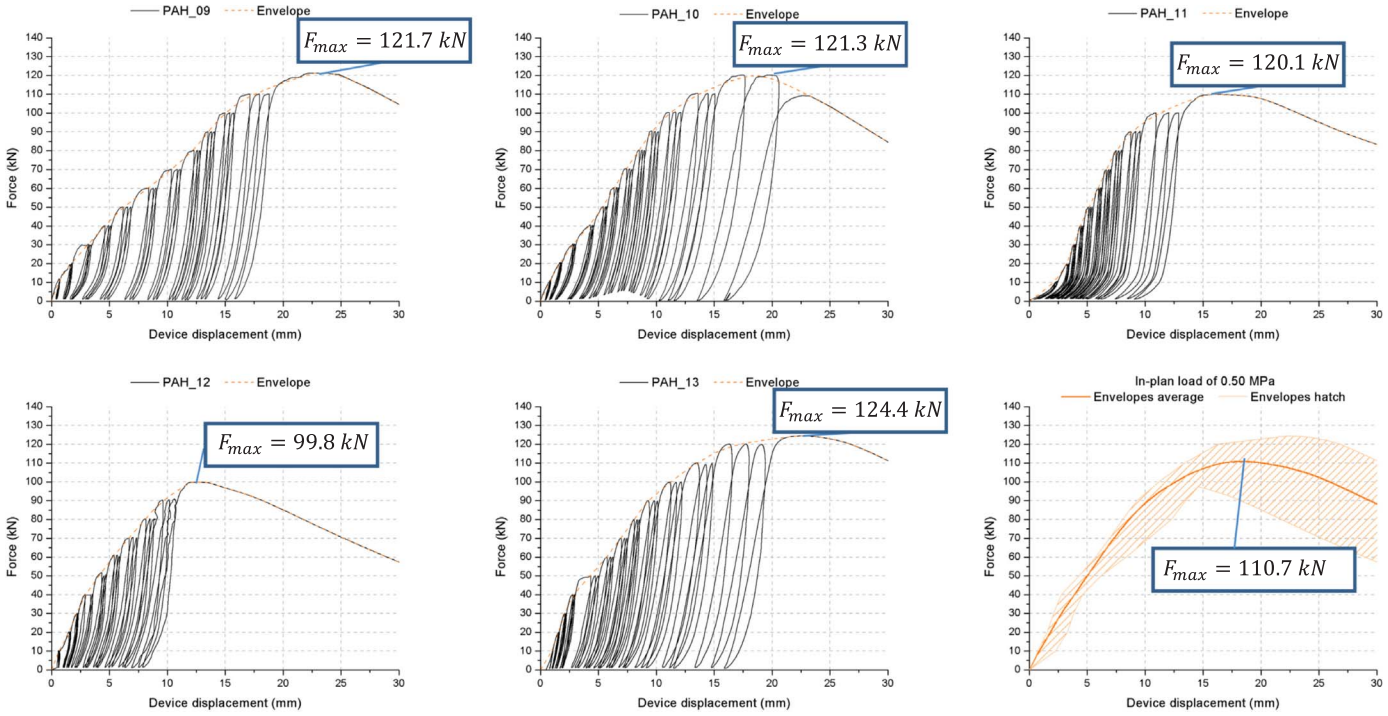

Fig. 16. Cyclic pull-out tests results (in-plane load of 240 kN/0.50 MPa).

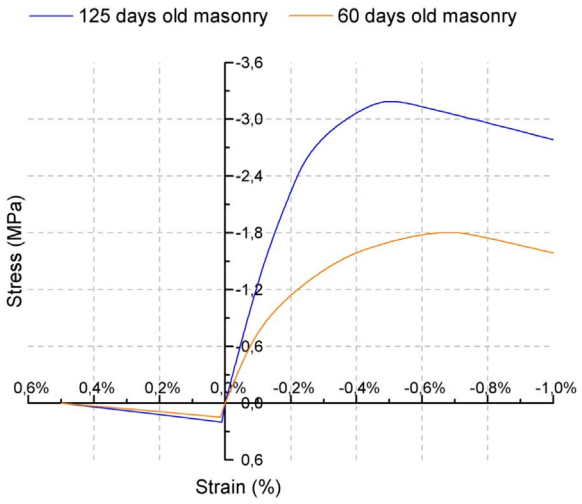

Fig. 17. Masonry uniaxial compressive strength.

$$F^2_{a,R}(h, \phi, \sigma_t, \sigma_n) = S_{cone}(h, \phi) \times \sigma_t \times \text{sen}\phi \times \lambda_1(\sigma_t, \sigma_n) \leq 200\,\text{kN} \quad (2)$$

Where the upper limit of 200 kN is the maximum strength of the anchoring system, the friction angle required in Eqs. (1) and (2) an angle measurement between 30° and 50° can be used for rubble stone masonry [19,21].

The parameter λ_1 can be computed by the Eq. (3), which was obtained on the assumption that the masonry compressive strength is about 10 times higher than the tensile strength (1/10 is a typical ratio for rubble stone masonry built with air lime mortars). The masonry tensile strength should be within the range of 0.10–0.30 MPa. The

Table 3
Numerical modellling distribution.

MODEL REF.	STUDY TYPE	AGE	APPLIED IN-PLANE LOAD	MAXIMUM PULL-OUT FORCE
MA_01	Experimental	60 days	0.21 MPa	106 kN
MA_02	modelling		0.50 MPa	116 kN
MA_03	Parametrical study	125 days	0.21 MPa	155 kN
MA_04			0.50 MPa	163 kN
MA_05		60 days	0.35 MPa	115 kN
MA_06		125 days		155 kN
MA_07		60 days	0.75 MPa	105 kN
MA_08		125 days		167 kN
MA_09		(125 +)	0.21 MPa	173 kN
MA_10		days	0.50 MPa	199 kN

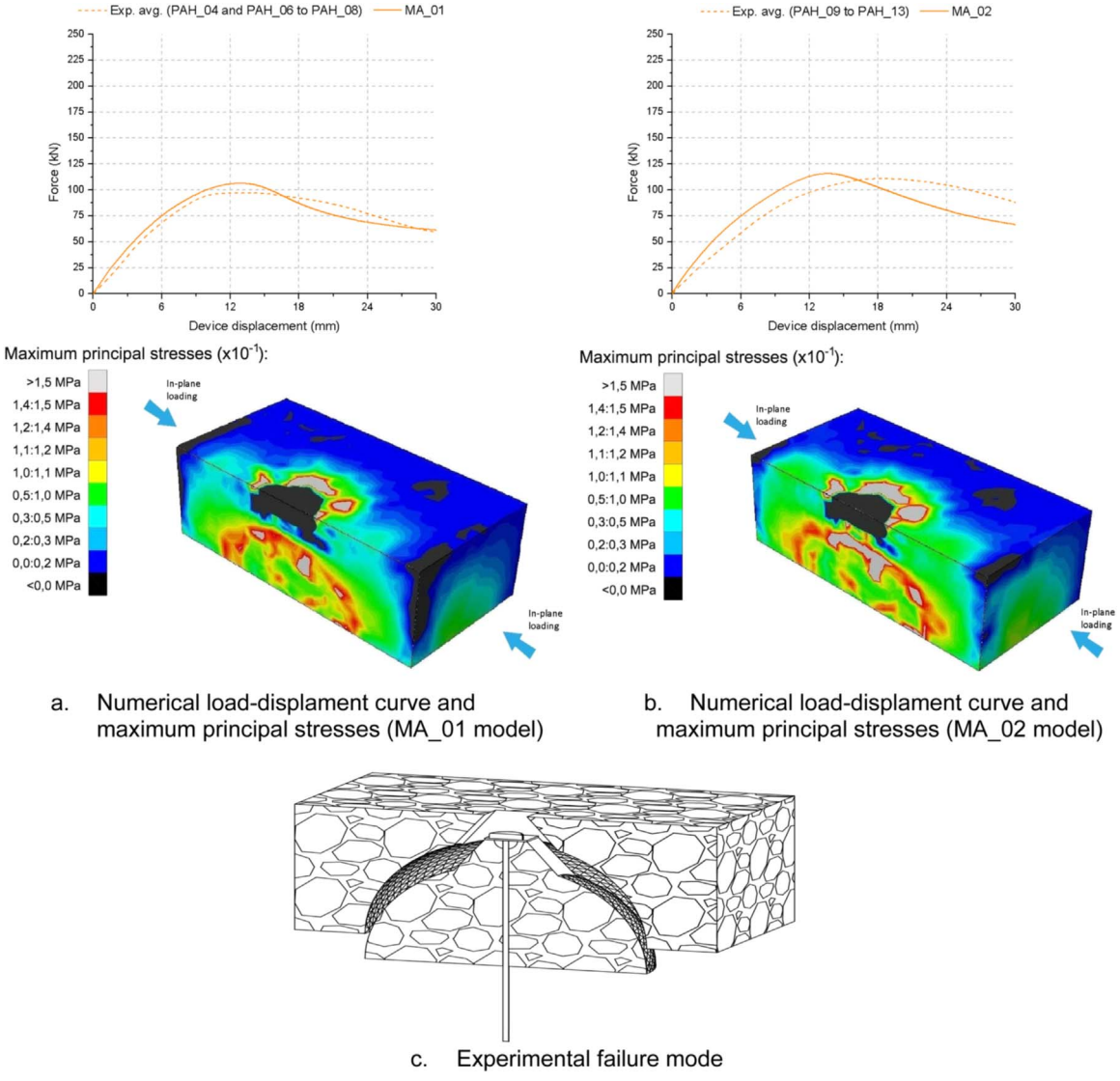

Fig. 18. Experimental modelling results.

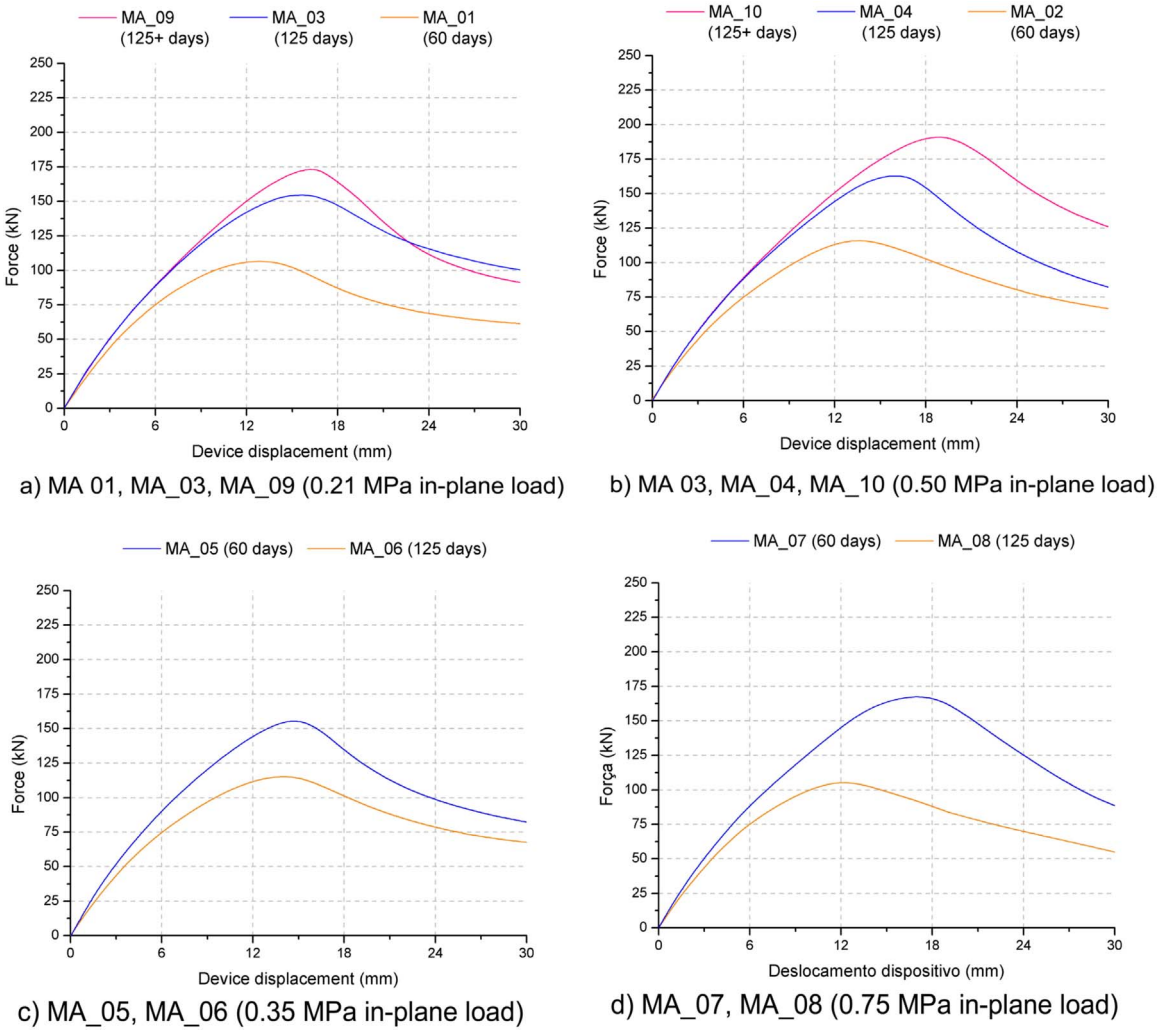

Fig. 19. Parametrical study results.

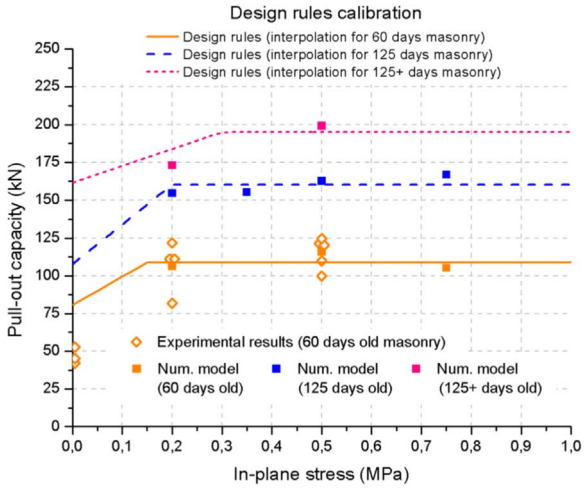

Fig. 20. Numerical and experimental concurrence to the design rules.

compressive stress on the wall (σ_n) is considered positive when in compression.

$$\begin{cases} \text{for } \sigma_n \le \sigma_t, \quad \lambda_1 = 1+(9,\ 50\cdot\sigma_t^{(1,5-4,4\cdot\sigma_t)}-1)\cdot\frac{\sigma_n}{\sigma_t} \\ \text{for } \sigma_n > \sigma_t, \qquad \lambda_1 = 9{,}50\cdot\sigma_t^{(1,5-4,4\cdot\sigma_t)} \end{cases} \tag{3}$$

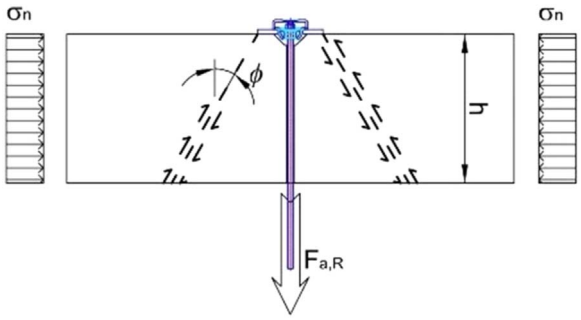

Fig. 21. Design rules variables.

Finally, the results showed that the anchoring system stiffness depends mainly on the system itself and on the tied rod deformability, meaning that the stiffness of the masonry and the level of the in-plane load is less relevant. From the experimental results, it was noted that the elastic anchoring system stiffness ($k_{anchoring\ sytem}$) can be expressed according to the length ($L_{tie\ rod}$), cross-section area (A) and Young modulus (E) of the tie rod:

$$\frac{1}{k_{anchoring\ sytem}} = \frac{1}{10\,000\ \text{to}\ 15\,000} + \frac{L_{tie\ rod}}{(EA)_{tie\ rod}} \left[\frac{m}{kN}\right] \tag{4}$$

8. Conclusions

The experimental and numerical testing procedures carried out, enabled us to understand the behaviour of the proposed anchoring system and the establishment of design rules for its pull-out capacity.

The proposed anchoring system has the advantage of allowing no-orthogonality between the system steel plate and the tie rod, being suitable for uneven connections between orthogonal walls and/or walls and floors. The experimental tests that were carried out showed that small angles (smaller than 20°) do not significantly change the system pull-out capacity.

The experimental testing process was preceded by an extensive characterization of the material to be used for purposes of testing model specimens, in order to obtain specimens similar to the traditional rubble stone masonry walls.

The masonry preliminary experimental characterization and the further pull-out tests enabled us to define an accurate model of finite elements, which was able to simulate the non-linear behaviour of the specimens and the punching shear surface generation.

In the pull-out experimental and numerical tests an important effect of the masonry strength and of the in-plane loading was observed. This has a significant confining effect on masonry. These effects were taken into account for purposes of defining the proposed design rules. With regard to these design rules, considered other meaningful effects on the design were also taken into consideration, such as, the thickness of the walls. Other issues, like the distance between devices for a group of anchors or boundary conditions, were not explicitly considered in the previous equations.

Acknowledgements

The authors gratefully acknowledge STAP, S.A, the promoter of the R & D project RehabToolBox, sponsored by FEDER through the POR Lisboa – QREN – Sistemas de Incentivos I & DT, for kindly granting the disclosure of the data presented in this paper.

The authors would like to thank the Ministério da Ciência, Tecnologia e Ensino Superior (Ministry of Science, Technology and Higher Education), FCT, Portugal [Grant number SFRH/BD/79339/2011].

References

[1] G. Magenes, A. Penna Existing masonry buildings: general code issues and methods of analysis and assessment, in: E. Cosenza (ed); Eurocode 8 Perspectives from the Italian Standpoint Workshop, Doppiavoce, Napoli, Italy, 2009, pp. 185–198.

[2] T. Johnson, R. Dowell, J. Silva, A review of code seismic demands for anchorage of nonstructural components, J. Build. Eng. 5 (2016) 249–253, http://dx.doi.org/10.1016/j.jobe.2015.11.002.

[3] J. Ingham, M. Griffith, Performance of unreinforced masonry buildings during the 2010 Darfield (Christchurch, NZ) earthquake, Aust. J. Struct. Eng. 11 (Iss. 3) (2010).

[4] F. Wenzel, H. Maus, Repair of masonry structures, Meccanica 27 (3) (1992) 223–232, http://dx.doi.org/10.1007/BF00430047.

[5] C. Modena, F. Da Porto, F. Casarin, M. Marco, S. Elena, Cultural heritage buildings and the Abruzzo earthquake: performance and post-earthquake actions, Adv. Mater. Res. 133–134 (2010) 623–628, http://dx.doi.org/10.4028/www.scientific.net/AMR.133-134.3.

[6] J. Ingham, D. Biggs, L. Moon, How did unreinforced masonry buildings perform in the February 2011 Christchurch earthquake? Struct. Eng. 89 (6) (2011) 14–18.

[7] J. Rondelet, Trattato teorico pratico sull'arte di edificare, Mantova (1834).

[8] E. Giuriani, G. Plizzari, C. Bassini, Experimental results on masonry wall anchored ties, WIT Trans. Built Environ. 39 (1999) 55–64 (ISSN: 1743-3509).

[9] T. Lin, J. LaFave, Experimental structural behavior of wall-diaphragm connections for older masonry buildings, Constr. Build. Mater. 26 (1) (2012) 180–189, http://dx.doi.org/10.1016/j.conbuildmat.2011.06.008.

[10] S. Paganoni, D. D'Ayala, Testing and design procedure for corner connections of masonry heritage buildings strengthened by metallic grouted anchors, Eng. Struct. 70 (2014) 278–293, http://dx.doi.org/10.1016/j.engstruct.2014.03.014.

[11] D. Reneckis, J. LaFave, W. Clarke, Out-of-plane performance of brick veneer walls on wood frame construction, Eng. Struct. 26 (8) (2004) 1027–1042, http://dx.doi.org/10.1016/j.engstruct.2004.02.013.

[12] S. Moreira, D. Oliveira, L. Ramos, P. Lourenço, R. Paula, J. Guerreiro, Experimental study on the seismic behavior of masonry wall-to-floor connections, in: Proceedings of the 15th World Conference on Earthquake Engineering (WCEE); Lisbon, 2012.

[13] S. Moreira, L. Ramos, D. Oliveira, P. Lourenço, Experimental behavior of masonry wall-to-timber elements connections strengthened with injection anchors, Eng. Struct. 81 (2014) 98–109, http://dx.doi.org/10.1016/j.engstruct.2014.09.034.

[14] ASTM E8 / E8M-11, Standard Test Methods for Tension Testing of Metallic Materials, ASTM International, 2011.

[15] EN 1926, Natural stone test methods - determination of uniaxial compressive strength, 2006.

[16] EN 1015-11, Methods of test for mortar for masonry – Part 11: determination of flexural and compressive strength of hardened mortar, 2006.

[17] A. Costigan, S. Pavía, O. Kinnane, An experimental evaluation of prediction models for the mechanical behaviour of unreinforced, lime-mortar masonry under compression, J. Build. Eng. 4 (2015) 283–294, http://dx.doi.org/10.1016/j.jobe.2015.10.001.

[18] EN 1052-1, Methods of test for masonry - Part 1: determination of compressive strength, 1998.

[19] J. Milosevic, M. Lopes, A. Gago, R. Bento, Testing and modelling the diagonal tension strength of rubble stone masonry panels, Eng. Struct. 52 (2013) 581–591, http://dx.doi.org/10.1016/j.engstruct.2013.03.019.

[20] J. Milosevic, A. Gago, M. Lopes, R. Bento, Experimental assessment of shear strength parameters on rubble stone masonry specimens, Constr. Build. Mater. 47 (2013) 1372–1380, http://dx.doi.org/10.1016/j.conbuildmat.2013.06.036.

[21] R. Pluijm, Out-of-Plane Bending of Masonry: Behavior and Strength (Ph.D. thesis), Eindhoven University of Technology, The Netherlands, 1999.